

Magnus spin Hall and spin Nernst effects in gapped 2D Rashba systems

Priyadarshini Kapri^{1,2}, Bashab Dey¹, and Tarun Kanti Ghosh¹

¹*Department of Physics, Indian Institute of Technology-Kanpur, Kanpur-208 016, India*

²*Department of Physics, Osaka University, Osaka-560 0043, Japan*

(Dated: July 20, 2022)

We study the Magnus transport in a gapped 2D electron gas with Rashba spin-orbit coupling using semiclassical Boltzmann transport formalism. Apart from its signature in the charge transport coefficients, the inclusion of Magnus velocity in the spin current operator enables us to study Magnus spin transport in the system. In particular, we study the roles of mass gap and Fermi surface topology on the behavior of Magnus Hall and Nernst conductivities and their spin counterparts. We find that the Magnus spin Hall conductivity vanishes in the limit of zero gap, unlike the universal spin Hall conductivity $\sigma_s = e/(8\pi)$. The Magnus spin currents with spin polarization perpendicular to the applied bias (electrical/thermal) are finite while with polarization along the bias vanishes. Each Magnus conductivity displays a plateau as Fermi energy sweeps through the gap and has peaks (whose magnitudes decrease with the gap) when the Fermi energy is at the gap edges.

I. INTRODUCTION

After the discovery of classical Hall effect, a wide range of Hall effects (HEs), such as quantum HE, anomalous HE, spin HE, nonlinear HE and thermal HE have been discovered in the course of time. These discoveries have played a leading role in elucidating the novel electronic states [1, 2] and electron dynamics [3, 4] and thus have drawn tremendous interest to the solid state community. The traditional (classical) Hall [3] effect and quantum Hall effect [1] arise only in the presence of an external magnetic field. However, anomalous [5–7] and the quantum anomalous Hall effect [8–10] originate from the anomalous velocity of the charge carriers, where the role of Berry curvature (BC) is involved. Further, the involvement of Berry curvature with spin index, valley index, and orbital degrees of freedom lead to the spin HE [11, 12], valley HE [13–15] and orbital HE [16, 17] respectively. Furthermore, the dipole moment of BC in momentum space generates a net anomalous velocity and gives rise to the non linear Hall effect [18]. Moreover, the thermal analogue of these Hall effects lead to thermal Hall effects [19, 20], which play a pivotal role in the field of caloritronics.

As we know, the discrete symmetries of the Hamiltonian namely, inversion symmetry (IS) and time reversal symmetry (TRS) play a significant role in directing the fate of the Hall current. For example, the intrinsic anomalous Hall effect (AHE) vanishes for TRS invariant systems, because the Berry curvature of the systems follows the relation: $\Omega(\mathbf{k}) = -\Omega(-\mathbf{k})$ and hence the Hall conductivity (which is proportional to the integral of Berry curvature) vanishes. However, such a distribution of Berry curvature in a TRS invariant system raises the question whether it can give rise to any interesting phenomena in charge transport. This leads to realization of the valley Hall effect [13] and the non-linear Hall effects in TRS invariant but IS broken systems [18, 20–22]. Very recently, it has been observed that such TRS invariant but IS broken systems with a built-in electric field and no external magnetic field manifests a new type

of Hall effect namely, Magnus Hall effect (MHE) [23]. The Magnus Hall effect represents the transverse force acting on a Bloch wave packet (having finite Berry curvature) moving under a potential gradient. To have the Magnus ‘force’ on an electron, it must have a finite Berry curvature, irrespective of the presence or absence of TRS.

In Refs. [24, 25] the appearance of Magnus Nernst effect (MNE) (transverse Magnus current produced by longitudinal thermal gradient) and Magnus thermal Hall effect (Magnus heat current in a direction transverse to a temperature gradient) are demonstrated in TRS invariant but inversion broken systems. It has been proposed that the systems having IS breaking and TRS invariant nature, such as, monolayer (ML) graphene on hBN, bilayer (BL) graphene with applied perpendicular electric field [26, 27], the two-dimensional (2D) transition metal dichalcogenides MX_2 ($M = Mo, W$ and $X = S, Se, Te$) [13, 28, 29], hetero-structures [30], surfaces of topological insulator (TI) [31] and Weyl semimetals [32–34] are the potential candidates for exploring the MHE and MNE. Thus, it remains to be seen whether the Magnus Hall effect and Magnus Nernst effect exist in systems where both the IS and TRS are broken with non zero Berry curvature.

Recently, in our previous paper [35], we have shown that the origin of the spin Hall current can be explained by redefining the spin current operator with inclusion of the anomalous velocity. We have also shown that the anomalous velocity can generate pure anomalous non linear spin current with in-plane polarization. Thus, our general instinct motivates us to investigate whether the inclusion of Magnus velocity in spin velocity operator can produce Magnus spin Hall current (out of plane polarization) and Magnus spin current (in-plane polarization). Also, the observation of Spin Nernst effect [36, 37] points towards a possibility of Magnus spin Nernst effect (MNE) on incorporation of the Magnus velocity.

Motivated by the above discussions, we study the Magnus Hall and the Magnus Nernst effect of a 2D Rashba system with mass gap that causes the TRS breaking of the system. In particular, we investigate the role of gap

parameter (induced by the TRS breaking gap term) and the role of Fermi surface topology in the behavior of Magnus Hall and the Magnus Nernst conductivities. Furthermore, we redefine the spin current operator with including the Magnus velocity and study the spin counterparts of Magnus conductivities. Our studies mainly emphasize on the results obtained using the conventional definition (with Magnus velocity) of spin current operator. A modified spin current operator was introduced in Ref.[38] which has a term representing spin torque in addition to the conventional terms of the spin current operator. We have also commented on the contribution of this additional term in the Magnus transport coefficients. It is to be noted that a lot of debates ensued regarding the definition of spin current operators [38–43]. Later, it was shown that in a spin non-conserving system, the equilibrium spin current and violation of the Onsager relation are intrinsic properties of spin transport irrespective of the definition of spin current operator [44].

This paper is organized as follows. In Sec. II A, we present the semiclassical Boltzmann transport formalism to discuss the Magnus Hall conductivities (MHCs) in the diffusive regime as well as in the ballistic regime. Section II B presents the extension of above theory to study spin counterparts of MHCs by inclusion of Magnus velocity in conventional spin velocity operator. Section III includes the basic information of a 2D gapped Rashba system. In Sec. IV, we present the analytical and numerical results. Finally Sec. V concludes and summarizes our main findings.

II. FORMALISM OF MAGNUS TRANSPORT

In this section, we present a theory for Magnus Hall, Magnus Nernst conductivities for a generic two-band system and finally extend the theory to calculate their spin counterparts.

A. Derivation of Magnus transport coefficients

A mesoscopic Hall bar is considered, where a slowly varying electric potential energy $U(r)$ is set along the length of the bar (See Fig. 1) The potential energy gradient is introduced by the two gate voltages, U_L and U_R . The difference in potential energies ($\Delta U = U_L - U_R$) gives rise to an in-built electric field $\mathbf{E}_{in} = e^{-1}\nabla_x U$ ($-e$ being the electronic charge) along the bar. Furthermore, an additional electric field \mathbf{E} (small bias), or temperature gradient ($\nabla_x T$) is applied between the source and drain.

As mentioned earlier, to have the Magnus transport, the material of the bar should have a non-zero Berry curvature $\mathbf{\Omega}$. The motion of wave-packet inside the Hall bar is described by the semiclassical equations of motion

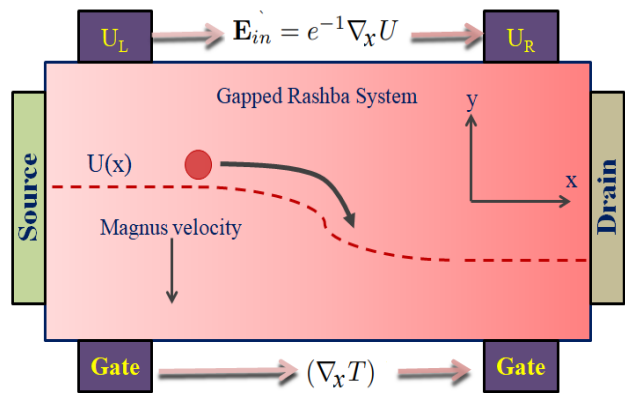


FIG. 1. Schematic illustration of the device for Magnus Hall effect. The difference in potential energies (induced by two gates) gives rise to an in-built electric field $\mathbf{E}_{in} = e^{-1}\nabla_x U$ along the bar. In presence of the in-built electric field, a self-rotating electron wave-packet (with a finite BC) that exits the source manifests a Magnus shift in transverse direction. An additional electric field \mathbf{E} , or temperature gradient ($\nabla_x T$) is applied between the source and drain.

[45, 46]

$$\hbar \dot{\mathbf{r}} = \nabla_{\mathbf{k}} \epsilon_{\mathbf{k}} + (\nabla_{\mathbf{r}} U + e\mathbf{E}) \times \mathbf{\Omega}, \quad (1)$$

$$\hbar \dot{\mathbf{k}} = -\nabla_{\mathbf{r}} U - e\mathbf{E}. \quad (2)$$

The first, second and third terms in the right hand side of Eq. (1) are associated with the semiclassical band velocity $\mathbf{v}_b = \frac{1}{\hbar}\nabla_{\mathbf{k}}\epsilon_{\mathbf{k}}$, Magnus velocity $\mathbf{v}_m = \frac{1}{\hbar}(\nabla_{\mathbf{r}}U \times \mathbf{\Omega})$ and anomalous velocity $\mathbf{v}_a = \frac{e}{\hbar}(\mathbf{E} \times \mathbf{\Omega})$, respectively with $\mathbf{\Omega}$ being the Berry curvature. For a 2D system confined in x - y plane, the Berry curvature is always in the \hat{z} -direction. Hence both the Magnus and the anomalous velocity are along the \hat{y} -direction because the in-built potential gradient and the external bias (electric field or temperature gradient) are along the \hat{x} direction.

Within the relaxation time approximation, the non-equilibrium carrier distribution function $f(\mathbf{r}, \mathbf{k})$ obeys the Boltzmann transport equation (BTE) [47]

$$\frac{\partial f}{\partial t} + \dot{\mathbf{r}} \cdot \frac{\partial f}{\partial \mathbf{r}} + \dot{\mathbf{k}} \cdot \frac{\partial f}{\partial \mathbf{k}} = -\frac{f - f_0}{\tau}, \quad (3)$$

where f_0 and τ denote the distribution function (in the presence of an inbuilt electric field) with no external bias and the scattering time, respectively. For simplicity, τ is considered to be momentum independent. In the steady state condition ($\frac{\partial f}{\partial t} = 0$), with no external bias the distribution function is given by the Fermi function

$$f_0(\mathbf{k}, \mathbf{r}) = \frac{1}{1 + e^{\beta[\epsilon(\mathbf{k}, \mathbf{r}) - \epsilon_F]}}, \quad (4)$$

where $\epsilon(\mathbf{k}, \mathbf{r}) = \epsilon_{\mathbf{k}} + U(\mathbf{r})$, $\beta = 1/k_B T$ and ϵ_F is a constant Fermi energy. Now, in the presence of an external

field (\hat{x} - directed), the distribution function up to first order in the bias fields can be obtained as

$$f = f_0 + v_{b,x}\tau(eE_x + \beta[\epsilon(\mathbf{k}, \mathbf{r}) - \epsilon_F]k_B\nabla_x T) \frac{\partial f_0}{\partial \epsilon_{\mathbf{k}}}, \quad (5)$$

where $v_{b,x}$ denotes the x component of band velocity v_b . For our setup, $v_x = v_{b,x}$, as both the anomalous and Magnus velocities are in \hat{y} direction.

In the presence of external electric field \mathbf{E} and temperature gradient ∇T applied between the source and drain, the charge current density \mathbf{J} from linear response theory can be written as

$$J_i = \sigma_{ij}E_j + \alpha_{ij}(-\nabla_j T), \quad (6)$$

where i and j denote the propagation and applied electric field directions with σ and α being the conductivity tensors. For our setup, $j = x$, as the external electric field or the temperature gradient is applied in \hat{x} direction.

For a two-band system, the general expression of charge current (considering all orders) in a 2D system can be written as

$$\mathbf{J} = -e \sum_{\lambda,n} \int \frac{d^2\mathbf{k}}{(2\pi)^2} \langle \lambda, \mathbf{k} | \hat{v} | \lambda, \mathbf{k} \rangle f_n, \quad (7)$$

where λ denotes the band index, f_n denotes the n -th order (n : order of extrinsic bias field) distribution function in the bias field and $\hat{v} = \hat{v}_b + \hat{v}_a + \hat{v}_m$ with \hat{v}_b , \hat{v}_a and \hat{v}_m being the band, anomalous and Magnus velocity operators. In Eq. (5), the first and second terms denote the distribution function with no external bias (f_0) and the first order distribution function in bias fields (f_1), respectively. From Eq. (7), one can easily separate out the band velocity (\hat{v}_b), anomalous velocity (\hat{v}_a) and the Magnus velocity (\hat{v}_m) contributions in the transport coefficients. Since the main focus of our paper is Magnus transport, we discuss the Magnus contribution only.

For an electric or thermal bias along x -direction, the Magnus Hall and Magnus Nernst currents of the first-order in bias field are given by $J_m = \sigma_m E_x$ and $J_m = -\alpha_m \nabla_x T$ respectively. The Magnus Hall (σ_m) and Magnus Nernst (α_m) conductivities in the diffusive limit can be written as

$$\sigma_m = -\frac{e^2 \Delta U}{\hbar L} \sum_{\lambda} \int \frac{d^2\mathbf{k}}{(2\pi)^2} \Omega_z^\lambda v_x^\lambda \tau_\lambda \frac{\partial f_0}{\partial \epsilon_{\mathbf{k}}}, \quad (8)$$

$$\alpha_m = \frac{e \Delta U}{\hbar L T} \sum_{\lambda} \int \frac{d^2\mathbf{k}}{(2\pi)^2} \Omega_z^\lambda v_x^\lambda \tau_\lambda \epsilon'_{\mathbf{k}} \frac{\partial f_0}{\partial \epsilon_{\mathbf{k}}}, \quad (9)$$

where $\langle \lambda, \mathbf{k} | \hat{v}_m | \lambda, \mathbf{k} \rangle = \frac{\partial U}{\partial x} \frac{\Omega_z^\lambda}{\hbar}$ and $f_1 = eE_x v_x^\lambda \tau_\lambda \frac{\partial f_0}{\partial \epsilon_{\mathbf{k}}}$ (driven by electric field) or $\frac{1}{T} v_x^\lambda \tau_\lambda \epsilon'_{\mathbf{k}} (\nabla_x T) \frac{\partial f_0}{\partial \epsilon_{\mathbf{k}}}$ (driven by temperature gradient, see Eq. 5)), U is a slowly varying function of x , $\partial U / \partial x = \Delta U / L$ with L being the length of the Hall bar and $\epsilon'_{\mathbf{k}} = (\epsilon_{\mathbf{k}} - \epsilon_F)$.

Here, it is to be noted that the Magnus conductivities of linear order (in external bias fields) arise from f_1 ,

whereas f_0 is responsible for first order anomalous conductivities as $\mathbf{v}_a \propto \mathbf{E}$. The Magnus conductivities can be viewed as an effective second order response as external bias and the built-in electric field both are involved in the calculation of currents.

So far the Magnus responses in the diffusive limit has been discussed. In the ideal ballistic regime, the mean free time between two collisions is infinite $\tau \rightarrow \infty$. In a realistic setup, the ballistic limit corresponds to the case where the mean free path is much larger than the system length i.e. $v_x \tau \gg L$. So, no collision occurs in the transport direction along the Hall bar. Therefore, the right hand side of the Boltzmann transport equation given in Eq. (3) vanishes in the ballistic regime.

In this setup, the larger electrochemical potential of the source region causes a surplus of electrons entering the system at $x = 0$ interface with $v_x > 0$. These electrons propagate across the device without any scattering in the ballistic limit. Hence, only the carriers from the source with positive velocity are allowed in region $0 < x < L$. Then, the the distribution function can be written as [23]

$$f_1(\mathbf{k}, \mathbf{r}) = -\Delta \epsilon_F \frac{\partial f_0}{\partial \epsilon_{\mathbf{k}}} - \frac{\epsilon'_{\mathbf{k}}}{T} \Delta T \frac{\partial f_0}{\partial \epsilon_{\mathbf{k}}} \quad \text{for } v_x > 0, \quad (10)$$

$$f_1(\mathbf{k}, \mathbf{r}) = 0 \quad \text{for } v_x < 0,$$

where $\Delta \epsilon_F = eV_{sd}$ is the electrochemical potential difference between the source and drain with V_{sd} being the small bias voltage. These solutions become identical with the solutions in Eq. (5), if one identifies the scattering length $v_x \tau = L$, $\Delta \epsilon_F / L = -eE_x$ and $\Delta T / L = -\nabla_x T$.

Thus, the linear order (in the bias field) Magnus Hall conductivity and the Magnus Nernst conductivity in the ballistic regime can be expressed as [23, 24]

$$\sigma_m = -\frac{e^2 \Delta U}{\hbar} \sum_{\lambda} \int_{v_x^\lambda > 0} \frac{d^2\mathbf{k}}{(2\pi)^2} \Omega_z^\lambda \frac{\partial f_0}{\partial \epsilon_{\mathbf{k}}}, \quad (11)$$

$$\alpha_m = \frac{e}{\hbar T} \Delta U \sum_{\lambda} \int_{v_x^\lambda > 0} \frac{d^2\mathbf{k}}{(2\pi)^2} \Omega_z^\lambda \epsilon'_{\mathbf{k}} \frac{\partial f_0}{\partial \epsilon_{\mathbf{k}}}. \quad (12)$$

As mentioned earlier, the Magnus responses are dependent on the built-in electric field.

In the following discussion, we elaborate the difference between anomalous and Magnus contributions. Under an inbuilt potential gradient ($\partial U / \partial x$) and applied source-drain bias (E_x) along x direction, the transverse charge current in the ballistic limit upto linear order in E_x is given by

$$J_y = \frac{e}{(2\pi)^2 \hbar} \sum_{\lambda} \left[-\int d^2\mathbf{k} f_0 \frac{\partial \epsilon_{\mathbf{k}}}{\partial k_y} + \int d^2\mathbf{k} f_0 \frac{\partial U}{\partial x} \Omega_z(\mathbf{k}) \right. \\ \left. + \int d^2\mathbf{k} f_0 eE_x \Omega_z(\mathbf{k}) - \int_{v_x > 0} d^2\mathbf{k} eE_x L \frac{\partial f_0}{\partial \epsilon_{\mathbf{k}}} \frac{\partial \epsilon_{\mathbf{k}}}{\partial k_y} \right. \\ \left. + \int_{v_x > 0} d^2\mathbf{k} eE_x L \frac{\partial f_0}{\partial \epsilon_{\mathbf{k}}} \frac{\partial U}{\partial x} \Omega_z(\mathbf{k}) \right]$$

The above expression contains five terms which are explained as follows: (i) The first term, representing *equilib-*

rium current due to band velocity, vanishes for every system. (ii) The second term denotes an *equilibrium Magnus current*, as it appears in the system without any bias voltage but only due to an intrinsic potential gradient. (iii) The third term represents the usual *anomalous Hall current* in response to the bias. In TRS invariant systems, the Berry curvature is an odd function in momentum space due to which its total over the entire Brillouin zone vanishes. As a result, a TRS invariant system produces no *equilibrium Magnus* or *anomalous Hall current*. However, for TRS broken systems, the *equilibrium Magnus* and *anomalous Hall currents* may be non-zero. (iv) The fourth term arises from the Fermi surface anisotropy and depends on its orientation relative to the direction of applied bias. (v) The fifth term represents the *Magnus Hall current* (equivalent to Eq. (11)). Since the integration is only over states with positive v_x , the *Magnus Hall current* may exist in TRS invariant systems under certain conditions i.e. tilt or anisotropy in the dispersion. In a TRS broken system with even function of Berry curvature such as the gapped Rashba system, the *Magnus Hall current* will always be non-zero. Thus, it may be finite in both TRS invariant and TRS broken systems. Since the TRS invariant systems do not have *equilibrium Magnus* or *anomalous Hall* contributions, the Magnus Hall current is of special interest in those cases. However, going by the above discussion, the TRS should not be a criteria to define the *Magnus Hall current*.

B. Derivation of Magnus spin conductivities

Now we extend the above theory to calculate the spin counterparts of the Magnus conductivities. The general definition of spin current (considering all orders in bias fields) for a 2D system can be written as

$$\mathcal{J}_{ij} = \frac{\hbar}{2} \sum_{\lambda, n} \int \frac{d^2 \mathbf{k}}{(2\pi)^2} \langle \lambda, \mathbf{k} | \hat{v}_{ij} | \lambda, \mathbf{k} \rangle f_n, \quad (14)$$

where $\hat{v}_{ij} = \hat{v}_{b,ij} + \hat{v}_{a,ij} + \hat{v}_{m,ij}$ with $\hat{v}_{b,ij}$, $\hat{v}_{a,ij}$, and $\hat{v}_{m,ij}$ being the band, the anomalous and the Magnus components of spin velocity operator, respectively. The first index i denotes the propagation direction and second index j denotes the polarization direction. Here, it is to be noted that the conventional definition of spin current operator is given by $\hat{v}_{b,ij} = (\hat{v}_{b,i}\sigma_j + \sigma_j\hat{v}_{b,i})/2$, with $\hat{v}_{b,i}$ being the band velocity operator in i direction. However, here the modified spin current operator contains both the anomalous and Magnus velocity contributions. As mentioned earlier, our main focus is on the Magnus transport. Thus, by separating out the Magnus contribution, the Magnus spin current of first order (in the bias fields) can be written as

$$\mathcal{J}_{m,ij} = \frac{\hbar}{2} \sum_{\lambda} \int \frac{d^2 \mathbf{k}}{(2\pi)^2} \langle \lambda, \mathbf{k} | \hat{v}_{m,ij} | \lambda, \mathbf{k} \rangle f_1. \quad (15)$$

with $f_1 = eE_x v_x^\lambda \tau_\lambda \frac{\partial f_0}{\partial \epsilon_{\mathbf{k}}}$ (driven by electric field) or $\frac{1}{T} v_x^\lambda \tau_\lambda \epsilon'_{\mathbf{k}} (\nabla_x T) \frac{\partial f_0}{\partial \epsilon_{\mathbf{k}}}$ (driven by temperature gradient, see Eq. 5).

From Eq. (15), one can easily find out the Magnus spin conductivity. In the diffusive regime, the \hat{x} directed electric field (external) driven Magnus spin conductivity ($\sigma_{m,yj} = \frac{\mathcal{J}_{m,yj}}{E_x}$) of first order with propagation and polarization in \hat{y} and \hat{j} directions, respectively, can be written as

$$\begin{aligned} \sigma_{m,yj} &= \frac{\hbar e}{2} \sum_{\lambda} \int \frac{d^2 \mathbf{k}}{(2\pi)^2} \tau_\lambda v_x^\lambda v_{m,yj}^\lambda \frac{\partial f_0}{\partial \epsilon_{\mathbf{k}}}, \quad (16) \\ &= \frac{e\Delta U}{2L} \sum_{\lambda} \int \frac{d^2 \mathbf{k}}{(2\pi)^2} \tau_\lambda v_x^\lambda \sigma_j^\lambda \Omega_z^\lambda \frac{\partial f_0}{\partial \epsilon_{\mathbf{k}}}, \end{aligned}$$

where $v_{m,yj}^\lambda = \langle \lambda, \mathbf{k} | \hat{v}_{m,yj} | \lambda, \mathbf{k} \rangle = \frac{1}{2} \langle \lambda, \mathbf{k} | \hat{v}_{m,y} \sigma_j | \lambda, \mathbf{k} \rangle = \frac{\Delta U \Omega_z^\lambda}{\hbar L} \sigma_j^\lambda$ with $\sigma_j^\lambda = \langle \lambda, \mathbf{k} | \sigma_j | \lambda, \mathbf{k} \rangle$.

Similarly, thermally driven first order Magnus spin conductivity ($\alpha_{m,yj} = \frac{\mathcal{J}_{m,yj}}{-\nabla_x T}$) propagating in \hat{y} direction with polarization in \hat{j} direction can be obtained as

$$\alpha_{m,yj} = -\frac{\Delta U}{2LT} \sum_{\lambda} \int \frac{d^2 \mathbf{k}}{(2\pi)^2} \tau_\lambda v_x^\lambda \sigma_j^\lambda \Omega_z^\lambda \epsilon'_{\mathbf{k}} \frac{\partial f_0}{\partial \epsilon_{\mathbf{k}}}. \quad (17)$$

For the ballistic regime, the Eq. (16) and Eq. (17) becomes

$$\sigma_{m,yj} = \frac{e\Delta U}{2} \sum_{\lambda} \int_{v_x^\lambda > 0} \frac{d^2 \mathbf{k}}{(2\pi)^2} \sigma_j^\lambda \Omega_z^\lambda \frac{\partial f_0}{\partial \epsilon_{\mathbf{k}}}, \quad (18)$$

$$\alpha_{m,yj} = -\frac{\Delta U}{2T} \sum_{\lambda} \int_{v_x^\lambda > 0} \frac{d^2 \mathbf{k}}{(2\pi)^2} \sigma_j^\lambda \Omega_z^\lambda \epsilon'_{\mathbf{k}} \frac{\partial f_0}{\partial \epsilon_{\mathbf{k}}}, \quad (19)$$

where $v_x^\lambda \tau_\lambda$ is replaced by L . Here, it is worth noting that $\sigma_{m,yz}$ and $\alpha_{m,yz}$ denote the Magnus spin Hall conductivity and Magnus spin Nernst conductivity, respectively (as the external bias field, propagation and polarization directions are mutually perpendicular to each other).

III. 2D GAPPED RASHBA SYSTEM

Here we provide the basic information of a gapped two-dimensional electron gas (2DEG) system with the Rashba spin-orbit interaction (RSOI). The Hamiltonian of the system is given by

$$H = \frac{\hbar^2 \mathbf{k}^2}{2m^*} \sigma_0 + \alpha \boldsymbol{\sigma} \cdot (\mathbf{k} \times \hat{\mathbf{z}}) + M\sigma_z, \quad (20)$$

where m^* denotes the effective mass of a charge carrier with $\mathbf{k} = \{k \cos \phi, k \sin \phi\}$ being the wavevector of the charge carrier, σ_0 is the 2×2 identity matrix, $\sigma_{x,y,z}$ are the Pauli's spin matrices and α is the RSOI strength which is responsible for inversion symmetry (IS) breaking of the system. The term $M\sigma_z$ breaks time reversal

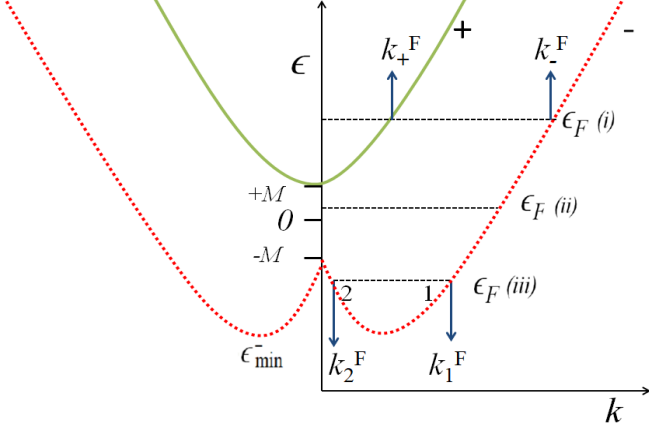


FIG. 2. Sketch of spin-split band structure of a 2D Rashba system with $M\sigma_z$, when $M < 2\epsilon_\alpha$ with $\epsilon_\alpha = m^*\alpha^2/(2\hbar^2)$. The band $\epsilon_+(\mathbf{k})$ has a minimum energy $\epsilon_{\min}^+ = +M$ located at $k = 0$ for all values of M , whereas the band $\epsilon_-(\mathbf{k})$ has a minimum energy $\epsilon_{\min}^- = -\epsilon_\alpha(1 + \tilde{M}^2)$ at $k_m = k_\alpha\sqrt{1 - \tilde{M}^2}$. It should be noted that expression for ϵ_{\min}^- is valid only when $\tilde{M} < 1$.

symmetry (TRS) of the system and can be created either by application of an external magnetic field [48] or by applying a circularly polarized electromagnetic radiation [49].

The energy spectrum of the system is obtained as

$$\epsilon_\lambda(\mathbf{k}) = \frac{\hbar^2 k^2}{2m^*} + \lambda\sqrt{M^2 + \alpha^2 k^2}, \quad (21)$$

with $\lambda = \pm$ denoting the band indices. The corresponding normalized wavefunctions are

$$|+, \mathbf{k}\rangle = \begin{bmatrix} \cos \frac{\theta}{2} e^{-i\phi} \\ -i \sin \frac{\theta}{2} \end{bmatrix}; \quad |-, \mathbf{k}\rangle = \begin{bmatrix} \sin \frac{\theta}{2} e^{-i\phi} \\ i \cos \frac{\theta}{2} \end{bmatrix}, \quad (22)$$

with $\cos \theta = M/\sqrt{M^2 + \alpha^2 k^2}$ and $\sin \theta = \alpha k/\sqrt{M^2 + \alpha^2 k^2}$. The TRS breaking term $M\sigma_z$ creates a finite gap $2M$ at $k = 0$. The spin orientation of an electron for this system is obtained as $\sigma^\lambda = \langle \lambda, \mathbf{k} | \boldsymbol{\sigma} | \lambda, \mathbf{k} \rangle = \lambda \{ \sin \theta \sin \phi, -\sin \theta \cos \phi, \cos \theta \}$.

The wavevectors corresponding to regime (i) ($\epsilon > M$, see Fig. 2) are $k_\lambda = k_\alpha \sqrt{(\tilde{E} - \lambda)^2 - \tilde{M}^2}$, with $\tilde{E} = \sqrt{1 + \tilde{\epsilon} + \tilde{M}^2}$, $\tilde{\epsilon} = \epsilon/\epsilon_\alpha$, $k_\alpha = m^*\alpha/\hbar^2$. The wavevectors k_\pm represent the radii of the two concentric circular constant energy contours of convex shape. For regime (iii) ($\epsilon < -M$ and $M < 2\epsilon_\alpha$), the topology of the Fermi surface has convex-concave shape on the outer and inner branches, respectively. Here, the wavevectors are presented by $k_\nu = k_\alpha \sqrt{[1 + (-1)^{\nu-1} \tilde{E}]^2 - \tilde{M}^2}$, where $\nu = 1, 2$ ($\nu = 1 \rightarrow$ outer branch and $\nu = 2 \rightarrow$ inner branch). For the regime regime (ii) ($-M \leq \epsilon \leq M$), only the branch $\nu = 1$ with $\lambda = -1$ exists.

For regime (i), the velocity component v_x corresponding to band λ is obtained as $v_x^\lambda = \frac{\hbar k_\alpha}{m^*} \tilde{E} \left[1 - \right.$

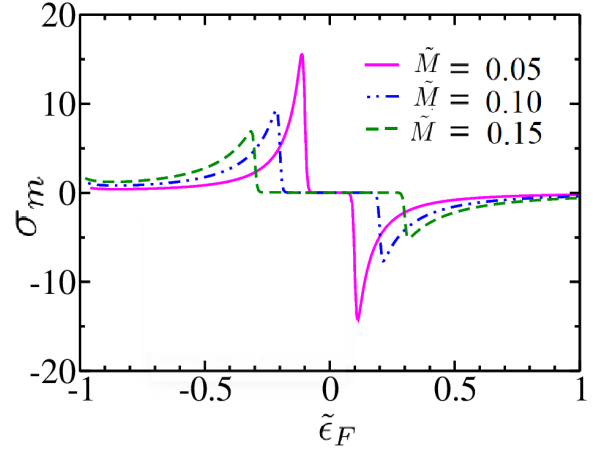


FIG. 3. The Magnus Hall conductivity σ_m (in units of σ_0) as a function of scaled Fermi energy $\tilde{\epsilon}_F$ for different values of \tilde{M} . Temperature is fixed at $T = 1$ K.

$\left. \frac{\tilde{M}^2}{(\tilde{E} - \lambda)^2} \right]^{1/2} \cos \phi$. This yields the limit of ϕ integration for calculating different Magnus conductivities in ballistic regime (see Eqs. (11-12) and Eqs. (18-19)). In the regime (iii), v_x can be obtained from the same equation with $\lambda = -1$ and \tilde{E} replaced by $(-1)^{\nu-1} \tilde{E}$. For the regime (ii), v_x has the similar form with $\nu = 1$.

The IS and TRS breaking terms give rise to a non zero Berry curvature in the system. The Berry curvature corresponding to band λ is given by

$$\Omega_\lambda(\mathbf{k}) = -\lambda \frac{M\alpha^2 \hat{\mathbf{z}}}{2(M^2 + \alpha^2 k^2)^{3/2}}, \quad (23)$$

which is isotropic in nature. It peaks at $k = 0$ and decays with increasing k . For a gapless 2D Rashba system, the Berry curvature and the orbital magnetic moment (OMM) are zero.

IV. RESULTS AND DISCUSSION

This section presents the results of different Magnus conductivities and their spin counterparts along with corresponding discussions. The plots for different conductivities are presented as a function of scaled Fermi energy $\tilde{\epsilon}_F$ ($\tilde{\epsilon}_F = \epsilon_F/\epsilon_\alpha$) for different values of dimensionless gap parameter \tilde{M} ($\tilde{M} = M/(2\epsilon_\alpha) = 0.05, 0.10, 0.15$). The temperature for all the plots is fixed at $T = 1$ K.

A. Electric field driven Magnus conductivity and Magnus spin conductivities

We calculate the Magnus Hall conductivity using Eq. (11). At zero temperature the Magnus Hall conductivity

in ballistic regime has the following forms

$$\begin{aligned}\sigma_m &= -\sigma_0 \frac{4\tilde{M}}{(\tilde{\epsilon}_F + \tilde{M}^2)^2} \text{ for regimes (i),} \\ \sigma_m &= \sigma_0 \frac{\tilde{M}}{\tilde{E}_F(\tilde{E}_F + 1)^2} \text{ for regime (ii),} \\ \sigma_m &= \sigma_0 \frac{2\tilde{M}(1 + \tilde{E}_F^2)}{\tilde{E}_F(\tilde{\epsilon}_F + \tilde{M}^2)^2} \text{ for regimes (iii),}\end{aligned}\quad (24)$$

where $\tilde{E}_F = \sqrt{1 + \tilde{\epsilon}_F + \tilde{M}^2}$ with $\tilde{\epsilon}_F = \epsilon_F/\epsilon_\alpha$ and $\sigma_0 = \frac{e^2}{\hbar} \frac{\Delta U}{16\pi\epsilon_\alpha}$.

It is to be noted that σ_m is discontinuous at $\epsilon_F = \pm M$. The reason is discussed below. The expression of σ_m (see Eq. 11) can be re written as $\sigma_m = -\frac{e^2\Delta U}{\hbar(2\pi)^2} \sum_\lambda \int_{-\infty}^{\infty} d\epsilon_k \mathcal{H}_\lambda(\epsilon_k) \frac{\partial f_0}{\partial \epsilon_k} \approx -\frac{e^2\Delta U}{\hbar(2\pi)^2} \sum_\lambda \mathcal{H}_\lambda(\epsilon_F)$, where $\mathcal{H}_\lambda(\epsilon) = \int_{v_x^{\lambda>0}} d\phi k_\lambda \frac{dk_\lambda}{d\epsilon_k} \Omega_z^\lambda$. Thus, the continuity of the Magnus Hall conductivity depends on the continuity of $\sum_\lambda \mathcal{H}_\lambda(\epsilon_F)$. From Fig. 2, it can be seen that ‘+’ band and branch ‘2’ of ‘-’ band are discontinuous at M and $-M$ respectively. Since $\mathcal{H}_+(\epsilon_F = M) \neq 0$ and $\mathcal{H}_{-,2}(\epsilon_F = -M) \neq 0$, σ_m becomes discontinuous at $\epsilon_F = \pm M$. It is worth mentioning that the linear Hall and spin Hall currents in a 2D gapped Rashba system are continuous at $\pm M$ [35, 48], although the integrands in their expressions are discontinuous at $\pm M$. This is because the linear Hall and spin Hall currents arise from f_0 (as opposed to $f_1 \propto \frac{\partial f_0}{\partial \epsilon} = -\delta(\epsilon - \epsilon_F)$ in Magnus Hall) due to which integration is performed from $-\infty$ to ϵ_F (at $T \rightarrow 0$) and not just the value of integrand at ϵ_F is picked up, as was the case with Magnus Hall current. For a 2D gapped system, similar to Magnus Hall current, non linear spin currents are also discontinuous at $\pm M$ because of the presence of f_1 in their definition.

It is worthwhile to mention that the asymmetric Berry curvature for right and left moving modes on the Fermi surface is necessary to have Magnus Hall effect only in TRS invariant materials with a broken inversion symmetry. This is to ensure a net non-zero Magnus contribution coming from the right movers. For example, in IS broken Dirac materials, the Berry curvatures have opposite signs in the two valleys due to TRS which makes it an odd function across the Brillouin zone. So, in absence of tilt or anisotropy in the dispersion, the number of right moving states at the Fermi pockets of both the valleys are equal and hence their Magnus contributions will cancel each other due to opposite signs of Berry curvature in the two valleys. However, the asymmetry is not necessary in the gapped Rashba system because it has only one valley and hence an isotropic Berry curvature is not a problem. Nevertheless, the Fermi contour of the system comprises of two concentric circles for $\epsilon_F < -M$ and $\epsilon_F > M$. For the former case, the Magnus contributions arising from the two branches of the ‘-’ band have the same sign and hence no cancellation takes place. For the latter case, the Magnus contributions arise from both the bands which have opposite signs of Berry curvature. Although the

signs of Magnus contributions of both the bands are opposite, they do not cancel each other because their magnitudes are different owing to the different Fermi wave vectors k_F^+ and k_F^- . Again, for $-M < \epsilon_F < M$, the Fermi contour of the system is a circle on the ‘-’ band. So, there is no question of cancellation of Magnus contribution because of the same sign on Berry curvature for all the states of the ‘-’ band. Thus, the Magnus effect is finite in the system despite an isotropic/symmetric Berry curvature. The Magnus contribution trivially vanishes as $M \rightarrow 0$ because the Berry curvature also vanishes in that limit.

The Magnus Hall conductivity σ_m (in units of $\sigma_0 = \frac{e^2}{\hbar} \frac{\Delta U}{16\pi\epsilon_\alpha}$) as a function of scaled Fermi energy $\tilde{\epsilon}_F$ for different values of \tilde{M} is shown in Fig. (3). Figure (3) depicts two peaks at the gap edges, i.e, at $\tilde{\epsilon}_F = \pm 2\tilde{M}$, where the magnitudes of the peaks decrease with the increasing strength of \tilde{M} . Furthermore, the Magnus Hall conductivity displays a plateau when Fermi energy lies between the two gap edges, i.e. $-2\tilde{M} < \tilde{\epsilon}_F < 2\tilde{M}$. For regime (i) and (iii), the Magnus Hall conductivity increases with \tilde{M} , which is opposite to the nature of variation of the peak values with M . Since, the Berry curvature decreases with momentum, Berry curvature for regime (iii) is greater than that for regime (i) (see Fig. 2). Thus, the magnitude of peak at $\tilde{\epsilon}_F = -2\tilde{M}$ is greater than that at $\tilde{\epsilon}_F = +2\tilde{M}$. Furthermore, the peaks have opposite signs.

Unlike the systems considered in previous works [23, 24], the gapped Rashba system has both *equilibrium Magnus* and *anomalous Hall currents* in addition to the Magnus Hall current (see Eq. (13)). The variation of *anomalous Hall current* with Fermi energy has already been studied for this system [45]. The *equilibrium Magnus current* is also expected to show similar trend of variation with Fermi energy as the *anomalous* one. Thus, in our work, we focus only on the Magnus Hall current. The fourth term in Eq.(13) vanishes for the gapped Rashba system, due to the isotropic nature of Fermi surface. In the gapped Rashba system, it is not possible to generate a pure Magnus Hall current. The Magnus Hall contribution can be isolated in an experiment by simply subtracting the Hall current measured without the inbuilt potential gradient from the Hall current obtained in presence of the gradient. However, the TRS invariant systems which exhibit Magnus Hall effect will have a pure Magnus current since their *equilibrium Magnus* and *anomalous Hall* contributions will vanish. The Magnus current can be identified from their peaks when the Fermi energy is at a gap edges. The tuning of the Fermi energy can be done by applying an overall gate potential in the experimental setup.

It is to be noted that in the diffusive regime, the Magnus Hall effect is equivalent to the nonlinear anomalous Hall effect arising due to Berry curvature dipole ($\partial_{k_x} \Omega_z$)[18]. This can be explained as follows. The nonlinear anomalous Hall current is given by $j_y = \sigma_{yxx} E_x^2$ where E_x is the electric field along x-direction and $\sigma_{yxx} \propto$

$\int \Omega_z(\partial_{k_x} f_0) d^2 \mathbf{k} = \int f_0(\partial_{k_x} \Omega_z) d^2 \mathbf{k}$ plus the boundary term. On decomposing E_x as $E_x = E_{in} + E_{ext}$, we get $E_x^2 = E_{in}^2 + 2E_{in}E_{ext} + E_{ext}^2$. The first term is second order in E_{in} , the second term corresponds to the Magnus contribution and the third term can be conventionally called as the *nonlinear anomalous Hall current* as it is proportional to square of the applied bias. Thus, the Magnus effect is a byproduct of nonlinear Hall effect when both internal and external fields are present. The origin of both effects are, however, the same i.e. Berry curvature dipole. In general, none of the three terms of the nonlinear Hall current can be neglected. It is only due to our intent of highlighting a Hall effect linear in E_{ext} that the E_{in}^2 and E_{ext}^2 contributions are disregarded. However, we have checked that the diffusive σ_{yxx} vanishes for the gapped Rashba system. Hence, all the three terms of the nonlinear Hall current identically vanish for this system in the diffusive regime.

The physics is slightly different in the ballistic regime. In this regime, the correction to distribution function is approximated to be independent of E_{in} because of the slow variation of the inbuilt potential. As a result, the nonlinear Hall current have contributions which go as $E_{in}E_{ext}$ and E_{ext}^2 only. Moreover, the nonlinear Hall current can no longer be written in terms of Berry curvature dipole by partial integration, because the form of correction to the distribution function for the ballistic case is different from the diffusive case. This can be shown as follows: In the diffusive regime,

$$\sigma_{yxx} \propto \iint_{\mathbf{k}} \Omega_z(\partial_{k_x} f_0) d^2 \mathbf{k} = \oint_{\Gamma} \Omega_z f_0 \hat{\mathbf{x}} \cdot \hat{\mathbf{n}} d\Gamma \quad (25)$$

$$- \iint_{\mathbf{k}} f_0(\partial_{k_x} \Omega_z) d^2 \mathbf{k},$$

where the last time on the right hand side corresponds to Berry curvature dipole. In the ballistic regime,

$$\sigma_{yxx} \propto \iint_{v_x > 0} \Omega_z(\partial_{k_x} f_0) d^2 \mathbf{k} \quad (26)$$

$$\propto \iint_{v_x > 0} \frac{\Omega_z}{v_x} (\partial_{k_x} f_0) d^2 \mathbf{k} = \oint_{\Gamma} \frac{\Omega_z}{v_x} f_0 \hat{\mathbf{x}} \cdot \hat{\mathbf{n}} d\Gamma$$

$$- \iint_{v_x > 0} f_0 \partial_{k_x} \left(\frac{\Omega_z}{v_x} \right) d^2 \mathbf{k}$$

Clearly, the last term in Eq.(26) is different from Berry curvature dipole. The constraint $v_x > 0$ in the integrals results in finite value of σ_{yxx} for the gapped Rashba system in the ballistic limit. In this limit, both $E_{in}E_{ext}$ and E_{ext}^2 contributions survive.

Now we calculate the spin counterpart of Magnus conductivity, i.e, Magnus spin conductivity for all polarization directions. The Magnus spin conductivities in ballistic regime are calculated using Eq. (18), where we find $\sigma_{m,yy} \neq 0$, $\sigma_{m,yz} \neq 0$ and $\sigma_{m,yx} = 0$. Thus, the Magnus spin conductivity having polarization in \hat{x} direction, i.e, $\sigma_{m,yx}$ vanishes, which can be explained using the angular integrals: $\sigma_{m,yx} \sim \int_{-\pi/2}^{\pi/2} \sin \phi d\phi$ or $\int_{\pi/2}^{3\pi/2} \sin \phi d\phi$,

depending on ϵ_F and λ . The $\sin \phi$ factor arises from σ_x^λ i.e. x -component of spin polarization. Both the integrals vanish, which is clearly a mathematical fact. Its physi-

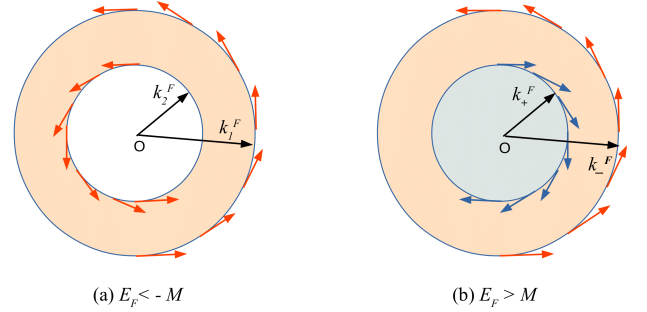


FIG. 4. Schematic representation of the in-plane component of spin-polarization vector (arrows) at points on the Fermi contours where $v_x > 0$ for (a) $E_F < -M$ and (b) $E_F > M$. The red and blue arrows are for ‘-’ and ‘+’ energy branches respectively.

cal origin can be explained as follows. From Eq. (18), we see that $\sigma_{m,yx}$ is proportional to the product of σ_x and Ω_z . Since Ω_z has same sign for all the states on either of the disjoint circles of the Fermi contour, the presence or absence of a net contribution to $\sigma_{m,yx}$ from each circle clearly depends on vector sum of x -component of spin-polarizations for states with $v_x > 0$. In the 2D Rashba system discussed in our manuscript, the spin-polarization vector is always perpendicular to the velocity of the electrons i.e. $(\hat{\sigma}^\lambda) \cdot \mathbf{v}^\lambda = 0$ (see Fig.4). Due to this arrangement, the x -component of spin polarizations on upper and lower halves of the contour cancel pairwise when summed over all states with $v_x > 0$. This accounts for the vanishing of $\sigma_{m,yx}$. However, this is not a universal feature. Had the Rashba interaction been of the form $\boldsymbol{\sigma} \cdot \mathbf{k}$, the spin-velocity locking would be of the form $(\hat{\sigma}^\lambda) \times \mathbf{v}^\lambda = 0$. In that case, the in-plane component of spin polarization vector will be parallel to the velocity. Under that arrangement, the Magnus spin conductivities with polarization along the bias would be finite and that perpendicular (in-plane) to it would vanish.

At zero temperature the Magnus spin conductivity having polarization in \hat{z} direction for ballistic regime is obtained as

$$\sigma_{m,yz} = \sigma_1 \frac{2\tilde{M}^2(\tilde{E}_F^2 + 3)}{(\tilde{\epsilon}_F + \tilde{M}^2)^3} \text{ for regime (i),} \quad (27)$$

$$\sigma_{m,yz} = \sigma_1 \frac{\tilde{M}^2}{\tilde{E}_F(\tilde{E}_F + 1)^3} \text{ for regime (ii),}$$

$$\sigma_{m,yz} = -\sigma_1 \frac{2\tilde{M}^2(3\tilde{E}_F^2 + 1)}{\tilde{E}_F(\tilde{\epsilon}_F + \tilde{M}^2)^3} \text{ for regime (iii),}$$

where $\sigma_1 = \frac{e}{32\pi} \frac{\Delta U}{\epsilon_\alpha}$. For $\sigma_{m,yz}$, the applied electric field, the propagation and polarization directions are mutually

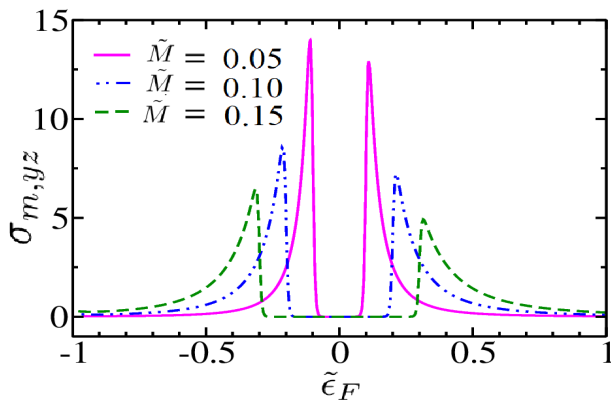


FIG. 5. The Magnus spin Hall conductivity $\sigma_{m,yz}$ (in units of σ_1) as a function of scaled Fermi energy $\tilde{\epsilon}_F$ for three different values of \tilde{M} . Temperature is fixed at $T = 1$ K.

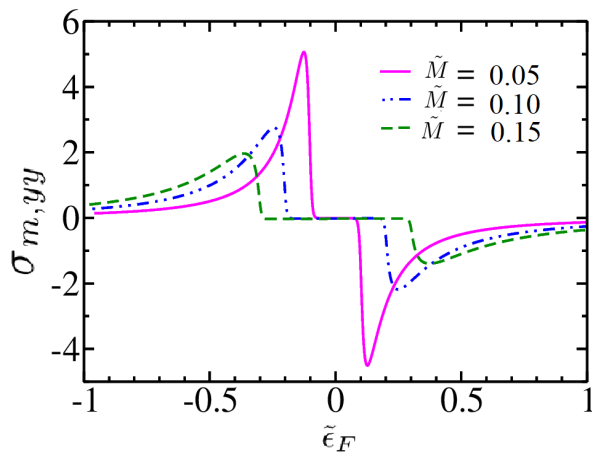


FIG. 6. The Magnus spin conductivity $\sigma_{m,yy}$ (in units of σ_1) as a function of $\tilde{\epsilon}_F$ for different values of \tilde{M} . Temperature is fixed at $T = 1$ K.

$$\sigma_{m,yy} = -\frac{2\sigma_1}{\pi} \frac{\tilde{M}}{\tilde{E}_F} \left[\frac{(\tilde{E}_F + 1)^3 [(\tilde{E}_F - 1)^2 - \tilde{M}^2]^{1/2} + (\tilde{E}_F - 1)^3 [(\tilde{E}_F + 1)^2 - \tilde{M}^2]^{1/2}}{(\tilde{\epsilon}_F + \tilde{M}^2)^3} \right] \text{ for regime (i) and (iii), (28)}$$

$$\sigma_{m,yy} = -\frac{2\sigma_1}{\pi} \frac{\tilde{M}}{\tilde{E}_F} \left[\frac{[(\tilde{E}_F + 1)^2 - \tilde{M}^2]^{1/2}}{(\tilde{E}_F + 1)^3} \right] \text{ for regime (ii).}$$

Figure 6 shows the Magnus spin conductivity $\sigma_{m,yy}$ (in units of σ_1) as a function of $\tilde{\epsilon}_F$ for different values of \tilde{M} . As expected, $\sigma_{m,yy}$ also shows the peaks at $\tilde{\epsilon}_F = \pm 2\tilde{M}$. Unlike the case of $\sigma_{m,yz}$, the peaks have opposite signs. As earlier, the peak magnitude decreases with \tilde{M} and for the regime (i) and (iii), the reverse nature is obtained.

perpendicular to each other and hence it can be called as Magnus spin Hall conductivity.

The Magnus spin Hall conductivity $\sigma_{m,yz}$ (in units of $\sigma_1 = \frac{e}{32\pi} \frac{\Delta U}{\epsilon_\alpha}$) as a function of $\tilde{\epsilon}_F$ for three different values of \tilde{M} is shown in Fig. 5. Figure 5 reveals that the Magnus spin Hall conductivity also has the peaks at the gap edges which have same signs unlike the Magnus Hall conductivity. Similar to σ_m , the magnitudes of the peaks decrease with \tilde{M} , but for regimes (i) and (iii), the magnitude of $\sigma_{m,yz}$ increases with M .

The gapped Rashba system has both spin Hall and Magnus spin Hall contributions. Both spin Hall and Magnus spin Hall effects arise on application of a source-drain bias (external field). But, to realize the latter, an inbuilt electric field is also required in addition to the bias. A finite Berry curvature is necessary for Magnus spin Hall effect, but not for spin Hall effect. Unlike the spin Hall conductivity which has a universal value $\sigma_s = \frac{e}{8\pi}$ for $M \rightarrow 0$ [11, 35], the Magnus spin Hall conductivity vanishes for $M \rightarrow 0$. This occurs due to the fact that the definition of spin Hall conductivity is weighted by zeroth order distribution function (f_0), whereas Magnus spin Hall conductivity is weighted by first order distribution function (f_1). In case of spin Hall conductivity, we need to perform the integration, where the upper limit yields $-\frac{e}{16\pi} \left[\frac{\tilde{M}^2}{(\tilde{E}_F - 1)^2} + \frac{M^2}{(\tilde{E}_F + 1)^2} \right]$ (which vanishes for $M \rightarrow 0$) and the lower limit of integration yields the universal value $\frac{e}{8\pi}$. On the contrary, for Magnus spin Hall conductivity, the integration yields the value of integrand at Fermi energy (because to the presence of first order distribution function ($f_1 \propto \frac{\partial f_0}{\partial \epsilon} = -\delta(\epsilon - \epsilon_F)$) which vanishes at $M \rightarrow 0$ (see Eq. (18) and Eq. (24)).

The Magnus spin conductivity $\sigma_{m,yy}$ having polarization in \hat{y} direction at zero temperature for ballistic regime is obtained as

B. Thermally driven Magnus conductivity and Magnus spin conductivities

In previous section, we have studied electric field (\hat{x} directed) driven Magnus conductivities, while this section presents the results of thermally driven (because of a temperature gradient ($\nabla_x T$) between the source and drain) Magnus conductivities.

First we calculate the Magnus Nernst conductivity

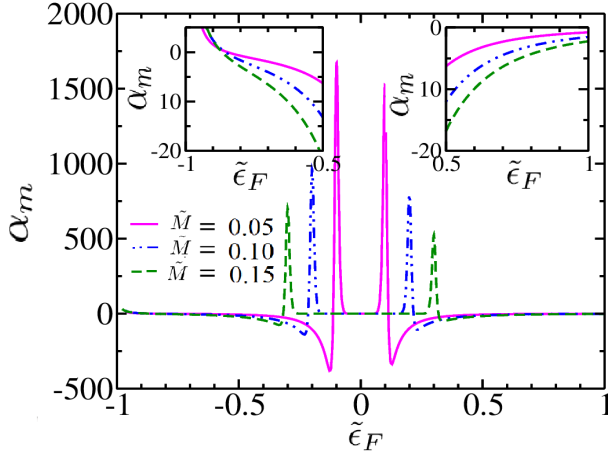


FIG. 7. The Magnus Nernst conductivity α_m (in units of α_0) as a function of scaled Fermi energy $\tilde{\epsilon}_F$ for different values of \tilde{M} . Temperature is fixed at $T = 1$ K.

(thermal analogue of Magnus Hall conductivity) using Eq. (12). In the limit $\epsilon_F \gg k_B T$, the Magnus Nernst conductivity for ballistic regime has the following forms

$$\begin{aligned} \alpha_m &= -\alpha_0 \frac{16\tilde{M}}{(\tilde{\epsilon}_F + \tilde{M}^2)^3} \text{ for regime (i)} \\ \alpha_m &= \alpha_0 \frac{\tilde{M}(1 + 3\tilde{E}_F)}{\tilde{E}_F^3(1 + \tilde{E}_F)^3} \text{ for regime (ii),} \\ \alpha_m &= \alpha_0 \frac{\tilde{M}(6\tilde{E}_F^4 + 12\tilde{E}_F^2 - 2)}{\tilde{E}_F^3(\tilde{\epsilon}_F + \tilde{M}^2)^3} \text{ for regime (iii),} \end{aligned} \quad (29)$$

where $\alpha_0 = \frac{e\Delta U \pi k_B^2 T}{96\hbar e^2 \epsilon_\alpha^2}$. Here, it is to be noted that the above expressions are valid for the Fermi energies away from the gap edges.

The Magnus Nernst conductivity α_m (in units of $\alpha_0 = \frac{e\Delta U \pi k_B^2 T}{96\hbar e^2 \epsilon_\alpha^2}$) as a function of scaled Fermi energy $\tilde{\epsilon}_F$ for different values of \tilde{M} is shown in Fig. (7). Unlike the previous cases, the peaks at the gap edges are accompanied by kinks, where the peak and kink values decrease with the increasing strength of \tilde{M} . The kinks in Fig. 7 can not be captured by the analytical expressions in Eq. (29). For each value of \tilde{M} , the plot displays nearly a plateau when Fermi energy lies inside the gap. For regime (i) (see right panel of insets) and (iii) (see left panel of insets), the Magnus Nernst conductivity increases with \tilde{M} . Unlike the Magnus Hall conductivity, the peaks for Magnus Nernst conductivity have same signs because of the term $\epsilon'_k = (\epsilon_k - \epsilon_F)$ in Eq. (12).

Now we present the results of thermally driven Magnus spin conductivities with different polarization in ballistic limit. Similar to the case of electric field driven Magnus spin conductivities, here also we find that Magnus spin conductivities having polarization in \hat{z} and \hat{y} directions are non zero, i.e. $\alpha_{m,yx} \neq 0$, $\alpha_{m,yz} \neq 0$, whereas

the Magnus spin conductivity having polarization in \hat{x} -

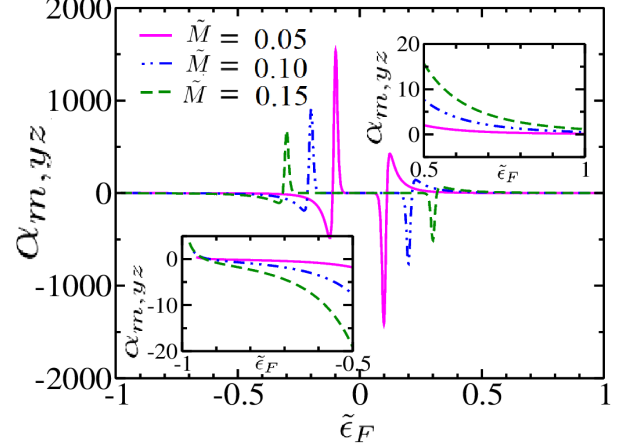


FIG. 8. The Magnus spin Nernst conductivity $\alpha_{m,yz}$ (in units of α_1) as a function of $\tilde{\epsilon}_F$ for different values of \tilde{M} . Temperature is fixed at $T = 1$ K.

direction ($\alpha_{m,yx}$) vanishes because of the ϕ integration. The physical reason is same as earlier.

In the limit $\epsilon_F \gg k_B T$, the thermally driven (for \hat{x} directed temperature gradient) Magnus spin conductivity with polarization in \hat{z} direction and propagation in \hat{y} direction for ballistic regime is obtained as

$$\begin{aligned} \alpha_{m,yz} &= \alpha_1 \frac{8\tilde{M}^2(\tilde{E}_F^2 + 5)}{(\tilde{\epsilon}_F + \tilde{M}^2)^4} \text{ for regime (i),} \\ \alpha_{m,yz} &= \alpha_1 \frac{\tilde{M}^2(4\tilde{E}_F + 1)}{\tilde{E}_F^3(\tilde{E}_F + 1)^4} \text{ for regime (ii),} \\ \alpha_{m,yz} &= -\alpha_1 \frac{2\tilde{M}^2(15\tilde{E}_F^4 + 10\tilde{E}_F^2 - 1)}{\tilde{E}_F^3(\tilde{\epsilon}_F + \tilde{M}^2)^4} \text{ for regime (iii),} \end{aligned} \quad (30)$$

where $\alpha_1 = \frac{\Delta U \pi k_B^2 T}{192e^2 \epsilon_\alpha^2}$. As earlier, these expressions are valid for the Fermi energies away from gap edges. This can be viewed as the thermal analogue of Magnus spin Hall conductivity, and hence called as Magnus spin Nernst conductivity.

Figure (8) depicts the Magnus spin Nernst conductivity $\alpha_{m,yz}$ (in units of $\alpha_1 = \frac{\Delta U \pi k_B^2 T}{192e^2 \epsilon_\alpha^2}$) as a function of $\tilde{\epsilon}_F$ for different values of \tilde{M} , where the peaks and kinks near the gap edges have opposite signs, unlike the cases of Magnus spin Hall conductivity $\sigma_{m,yz}$ and Magnus Nernst conductivity α_m . As expected, the behavior of $\alpha_{m,yz}$ as a function of \tilde{M} is similar as earlier, i.e, the peak and kink values decrease with increasing strength of \tilde{M} and the opposite trend is obtained for the regime (i) (see right panel of insets) and (iii) (see left panel of insets).

Now, in the limit $\epsilon_F \gg k_B T$ and for the Fermi energies away from the gap edges, the thermally driven Magnus spin conductivity with polarization and propagation in \hat{y} direction for ballistic regime has the following forms

$$\alpha_{m,yy} = \frac{2\alpha_1}{\pi} \frac{\tilde{M}}{\tilde{E}_F^3} \sum_{\eta=\pm} \frac{(-3\tilde{E}_F^3 + \eta 7\tilde{E}_F^2 - 5\tilde{E}_F + 4\tilde{M}^2\tilde{E}_F + \eta - \eta\tilde{M}^2)}{[(\tilde{E}_F - \eta)^2 - \tilde{M}^2]^{1/2}(\tilde{E}_F - \eta)^4} \text{ for regimes (i) and (iii),} \quad (31)$$

$$\alpha_{m,yy} = \frac{2\alpha_1}{\pi} \frac{\tilde{M}}{\tilde{E}_F^3} \frac{(-3\tilde{E}_F^3 - 7\tilde{E}_F^2 - 5\tilde{E}_F + 4\tilde{M}^2\tilde{E}_F - 1 + \tilde{M}^2)}{[(\tilde{E}_F + 1)^2 - \tilde{M}^2]^{1/2}(\tilde{E}_F + 1)^4} \text{ for regime (ii).}$$

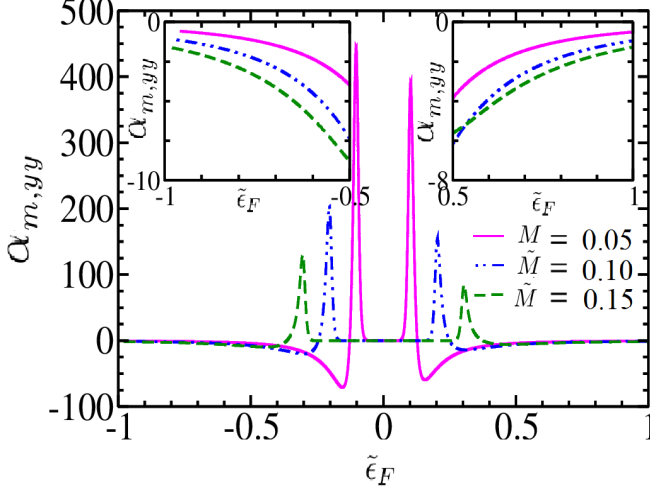


FIG. 9. The thermally driven Magnus spin conductivity $\alpha_{m,yy}$ (in units of α_1) as a function of $\tilde{\epsilon}_F$ for different values of \tilde{M} . Temperature is fixed at $T = 1$ K.

The thermally driven Magnus spin conductivity $\alpha_{m,yy}$ (in units of α_1) as a function of $\tilde{\epsilon}_F$ for different values of \tilde{M} is shown in Fig. 9. Figure 9 reveals that $\alpha_{m,yy}$ also has the peaks and kinks at around the gap edges with the peaks and kinks having same signs. Insets of Fig. 9 depict the behavior of $\alpha_{m,yy}$ in the regime (i) and (iii), where it is clear that the magnitude of $\alpha_{m,yy}$ increases with \tilde{M} , though the changes are small.

It is to be noted that all the results presented in our manuscript are for ballistic regime only ($v_x\tau \gg L$). We have checked that the minimum value of $v_x\tau$ (where τ is energy dependent) for $\phi = 0$, $\alpha = 0.1$ eV nm, $m^* = 0.3 m_e$ and $\tau_0 = 2.5$ ps is ~ 20 nm. So, our calculations for ballistic regime are valid when the system length (L) is few nanometers.

There are some qualitative differences between Magnus spin Hall and Nernst effects in the diffusive (i.e. in presence of impurities) and the ballistic regime. In the ballistic regime, only the carriers having $v_x > 0$ on the Fermi contour contribute while in the diffusive regime, all the states on the Fermi contour contribute. The diffusive conductivities have an additional factor $v_x\tau$ in the integrand. In the ballistic limit, $\sigma_{m,yz}, \sigma_{m,yy} \neq 0$ and $\sigma_{m,yx} = 0$. However, in the diffusive regime, we find that $\sigma_{m,yz}$ ($\propto \int_0^{2\pi} \cos \phi d\phi = 0$) does not survive, $\sigma_{m,yx}$ ($\propto \int_0^{2\pi} \cos \phi \sin \phi d\phi = 0$) still remains zero and

$\sigma_{m,yy}$ ($\propto \int_0^{2\pi} \cos^2 \phi d\phi \neq 0$) gets renormalized by a factor in regimes (i) and (ii) but has a modified expression in regime (iii). The reason is as follows: for regime (iii), the contributions of $\nu = 2$ branch have opposite signs for ballistic ($\sigma_{m,yy} \propto \int_{\pi/2}^{3\pi/2} \cos \phi d\phi$) and diffusive regimes ($\sigma_{m,yy} \propto \int_0^{2\pi} \cos^2 \phi d\phi$). We have also checked that $\sigma_{m,yy}$ with k -dependent τ shows qualitatively similar trend of variation with Fermi energy as that with constant τ . Thus, in presence of impurities, only the Magnus spin conductivities with an in-plane polarization transverse to the bias is present for the gapped Rashba system. Similar behavior is obtained by the Magnus Nernst conductivities.

As mentioned earlier, our results are presented with the conventional definition of spin current operator. With the modified definition of spin current operator of Ref. [38], we find that the additional term in spin current operator ($\hat{r}(d\hat{s}_z/dt)$) has no contribution to $\sigma_{m,yz}$, because the torque density trivially vanishes for all states i.e. $\mathcal{T}_z(\mathbf{r}) = (1/i\hbar)Re\Psi^\dagger(\mathbf{r})[\hat{\sigma}_z, \hat{H}]\Psi(\mathbf{r}) = 0$. Similarly, we find that $\mathcal{T}_y(\mathbf{r}) = (1/i\hbar)Re\Psi^\dagger(\mathbf{r})[\hat{\sigma}_y, \hat{H}]\Psi(\mathbf{r}) = \mathcal{T}_x(\mathbf{r}) = (1/i\hbar)Re\Psi^\dagger(\mathbf{r})[\hat{\sigma}_x, \hat{H}]\Psi(\mathbf{r}) = 0$. Thus, $\sigma_{m,yj}$ presented in our manuscript remain same with the new definition of spin current operator. It is worthwhile to mention that many works on spin current [50–52] have been carried out with the conventional definition of spin current operator.

V. CONCLUSION

In this paper, we have explored the Magnus transport in a system, where both the inversion symmetry and time reversal symmetry are broken with a finite Berry curvature. The Magnus Hall effect arises because of the Magnus velocity which appears in a self-rotating quantum electronic wave-packet moving through a crystalline material having potential energy gradient. We have studied both the electric field driven and temperature gradient driven Magnus conductivities in a gapped 2D Rashba system in ballistic regime. The spin counterparts of the Magnus conductivities have also been explored by modifying the spin current operator with inclusion of the Magnus velocity. Unlike the spin Hall conductivity which has a universal value $\sigma_s = \frac{e}{8\pi}$ as $M \rightarrow 0$, the Magnus spin Hall conductivity vanishes in this limit. We have found that the Magnus spin currents with spin polarization perpendicular to the applied bias (electrical/thermal) are finite while with polarization along the bias vanishes because of the ϕ integration. We have studied the role of

gap parameter (M , induced by the time reversal symmetry breaking term) and the Fermi energy (ϵ_F) on the behavior of different conductivities. We find that all the conductivities and their spin counterparts show peaks (and kinks for thermally driven conductivities) at the gap edges, where magnitudes of peaks (and kinks) decrease with the increasing strength of gap parameter. For the regime $\epsilon_F > M$ and $\epsilon_F < -M$, the conductivities increase with increasing strength of M . All the Magnus conductivities are nearly constant when the Fermi energy

varies inside the gap.

VI. ACKNOWLEDGMENT

P. Kapri thanks Department of Physics, IIT Kanpur, India and Department of Physics, Osaka University, Japan.

-
- [1] K. V. Klitzing, G. Dorda, and M. Pepper, *Phys. Rev. Lett.* **45**, 494 (1980).
- [2] F. D. M. Haldane, *Phys. Rev. Lett.* **61**, 2015 (1988).
- [3] E. H. Hall, *Am. J. Math.* **2**, 287 (1879).
- [4] R. Karplus and J. M. Luttinger, *Phys. Rev.* **95**, 1154 (1954).
- [5] E. H. Hall, *The London, Edinburgh, and Dublin Philosophical Magazine and Journal of Science* **10**, 301 (1880).
- [6] N. A. Sinitsyn, *J. Phys. Condens. Matter* **20**, 023201 (2008).
- [7] N. Nagaosa, J. Sinova, S. Onoda, A. H. MacDonald, and N. P. Ong, *Rev. Mod. Phys.* **82**, 1539 (2010).
- [8] C. Z. Chang, J. Zhang, X. Feng, J. Shen, Z. Zhang, M. Guo, K. Li, Y. Ou, P. Wei, L. L. Wang, Z. Q. Ji, Y. Feng, S. Ji, X. Chen, J. Jia, X. Dai, Z. Fang, S. C. Zhang, K. He, Y. Wang, L. Lu, X. Ma, and Q. K. Xue, *Science* **340**, 167 (2013).
- [9] C. X. Liu, S. C. Zhang, and X. L. Qi, *Annu. Rev. Condens. Matter Phys.* **7**, 301 (2016).
- [10] K. He, Y. Wang, and Q. K. Xue, *Annu. Rev. Condens. Matter Phys.* **9**, 329 (2018).
- [11] J. Sinova, D. Culcer, Q. Niu, N. A. Sinitsyn, T. Jungwirth, and A. H. MacDonald, *Phys. Rev. Lett.* **92**, 126603 (2004).
- [12] J. Sinova, S. O. Valenzuela, J. Wunderlich, C. H. Back, and T. Jungwirth, *Rev. Mod. Phys.* **87**, 1213 (2015).
- [13] D. Xiao, W. Yao, and Q. Niu, *Phys. Rev. Lett.* **99**, 236809 (2007).
- [14] D. Xiao, G. B. Liu, W. Feng, X. Xu, and W. Yao, *Phys. Rev. Lett.* **108**, 196802 (2012).
- [15] K. F. Mak, K. L. McGill, J. Park, and P. L. McEuen, *Science* **344**, 1489 (2014).
- [16] D. Go, D. Jo, C. Kim, and H. W. Lee, *Phys. Rev. Lett.* **121**, 086602 (2018).
- [17] L. M. Canonico, T. P. Cysne, T. G. Rappoport, and R. B. Muniz, *Phys. Rev. B* **101**, 075429 (2020).
- [18] I. Sodemann and L. Fu, *Phys. Rev. Lett.* **115**, 216806 (2015).
- [19] X. Q. Yu, Z. G. Zhu, G. Su, and A. P. Jauho, *Phys. Rev. Lett.* **115**, 246601 (2015).
- [20] T. Liang, J. Lin, Q. Gibson, T. Gao, M. Hirschberger, M. Liu, R. J. Cava, and N. P. Ong, *Phys. Rev. Lett.* **118**, 136601 (2017).
- [21] T. Morimoto and N. Nagaosa, *Sci. Adv.* **2**, e1501524 (2016).
- [22] S. Nandy and I. Sodemann, *Phys. Rev. B* **100**, 195117 (2019).
- [23] M. Papaj and L. Fu, *Phys. Rev. Lett.* **123**, 216802 (2019).
- [24] D. Mandal, K. Das, and A. Agarwal, *Phys. Rev. B* **102**, 205414 (2020).
- [25] S. K. Das, T. Nag, and S. Nandy, *Phys. Rev. B* **104**, 115420 (2021).
- [26] E. McCann and M. Koshino, *Rep. Prog. Phys.* **76**, 056503 (2013).
- [27] A. V. Rozhkov, A. O. Sboychakov, A. L. Rakhmanov, and F. Nori, *Phys. Rep.* **648**, 1 (2016).
- [28] X. Qian, J. Liu, L. Fu, and J. Li, *Science* **346**, 1344 (2014).
- [29] J.-S. You, S. Fang, S.-Y. Xu, E. Kaxiras, and T. Low, *Phys. Rev. B* **98**, 121109 (2018).
- [30] M. Yankowitz, J. Xue, D. Cormode, J. D. Sanchez-Yamagishi, K. Watanabe, T. Taniguchi, P. Jarillo-Herrero, P. Jacquod, and B. J. LeRoy, *Nat. Phys.* **8**, 382 (2012).
- [31] L. Fu, *Phys. Rev. Lett.* **103**, 266801 (2009).
- [32] M. Z. Hasan, S.-Y. Xu, I. Belopolski, and S.-M. Huang, *Annu. Rev. Condens. Matter Phys.* **8**, 289 (2017).
- [33] N. P. Armitage, E. J. Mele, and A. Vishwanath, *Rev. Mod. Phys.* **90**, 015001 (2018).
- [34] B. Yan and C. Felser, *Annu. Rev. Condens. Matter Phys.* **8**, 337 (2017).
- [35] P. Kapri, B. Dey, and T. K. Ghosh, *Phys. Rev. B* **103**, 165401 (2021).
- [36] S. Meyer, Y.-T. Chen, S. Wimmer, M. Althammer, T. Wimmer, R. Schlitz, S. Geprags, H. Huebl, D. Kodderitzsch, H. Ebert, G. E. W. Bauer, R. Gross and S. T. B. Goennenwein, *Nat. Mater.* **16**, 977 (2017).
- [37] P. Sheng, Y. Sakuraba, Y. C. Lau, S. Takahashi, S. Mitani, and M. Hayash, *Sci. Adv.* **3**, 1701503 (2017).
- [38] J. Shi, P. Zhang, D. Xiao, and Q. Niu, *Phys. Rev. Lett.* **96**, 076604 (2006).
- [39] E. I. Rashba, *Phys. Rev. B* **68**, 241315 (2003).
- [40] E. I. Rashba, *Phys. Rev. B* **70**, 161201(R) (2004).
- [41] Q.-F. Sun and X. C. Xie, *Phys. Rev. B* **72**, 245305 (2005).
- [42] Y. Wang, K. Xia, Z.-B. Su, and Z. Ma, *Phys. Rev. Lett.* **96**, 066601 (2006).
- [43] J. Wang, B. Wang, W. Ren, and H. Guo, *Phys. Rev. B* **74**, 155307 (2006).
- [44] Q. Sun, X. C. Xie, and J. Wang, *Phys. Rev. B* **77**, 035327 (2008).
- [45] D. Xiao, M.-C. Chang, and Q. Niu, *Rev. Mod. Phys.* **82**, 1959 (2010).
- [46] D. T. Son and N. Yamamoto, *Phys. Rev. Lett.* **109**, 181602 (2012).
- [47] N.W. Ashcroft and N.D. Mermin, *Solid State Physics, HRW international editions (Holt, Rinehart and Winston)*, (1976).

- [48] D. Culcer, A. MacDonald, and Q. Niu, Phys. Rev. B **68**, 045327 (2003).
- [49] T. Ojanen and T. Kitagawa, Phys. Rev. B **85**, 161202(R) (2012).
- [50] E. B. Sonin, Phys. Rev. Lett. **99**, 266602 (2007).
- [51] K. Hamamoto, M. Ezawa, K. W. Kim, T. Morimoto, and N. Nagaosa, Phys. Rev. B **95**, 224430 (2017).
- [52] A. Pan and D. C. Marinescu, Phys. Rev. B **99**, 245204 (2019).